Oxidative and Salt Stresses Alter the 26S Proteasome Holoenzyme and Associated Protein Profiles in Arabidopsis Thaliana

Diana Bonea
University of Toronto
Jenan Noureddine
University of Toronto
Sonia Gazzarrini
University of Toronto
Rongmin Zhao (RONGMIN.ZHAO@UTORONTO.CA)
University of Toronto

Research Article

Keywords: 26S proteasome, abiotic stresses, assembly chaperone, molecular chaperone, plant stress response, proteasome assembly, protein homeostasis, protein degradation

Posted Date: June 4th, 2021

DOI: https://doi.org/10.21203/rs.3.rs-555980/v1

Abstract

Background: The 26S proteasome, canonically composed of multi-subunit 19S regulatory (RP) and 20S core (CP) particles, is crucial for cellular proteostasis. Proteasomes may be re-modeled, activated, or re-localized and this regulation is critical for plants in response to environmental stresses. The proteasome holoenzyme assembly and dissociation are therefore highly dynamic in vivo. However, the stoichiometric changes of the plant proteasomes and how proteasome associated chaperones vary under common abiotic stresses have not been systematically studied.

Results: Here, we studied the impact of abiotic stresses on proteasome structure, activity, and interacting partners in *Arabidopsis thaliana*. We analyzed available RNA expression data and observed that expressions of proteasome coding genes varied substantially under stresses; however, the protein levels of a few key subunits did not change significantly within 24 hours. Instead, a switch in the predominant proteasome complex, from 26S to 20S, occurs under oxidative or salt stress. Oxidative stress also reduced the cellular ATP content and the association of HSP70-family proteins to the 20S proteasome, but enhanced the activity of cellular free form CP. Salt stress, on the other hand, did not affect cellular ATP level, but caused subtle changes in proteasome subunit composition and impacted bindings of assembly chaperones. Analyses of an array of T-DNA insertional mutant lines highlighted important roles for several putative assembly chaperones in seedling establishment and stress sensitivity. We also observed that knockout of PBAC1, one of the a-ring assembly chaperones, resulted in hypersensitivity and tearing of the seed coat during sterilization.

Conclusions: Our study revealed an evolutionarily conserved mechanism of proteasome regulation during oxidative stress, involving dynamic regulation of the holoenzyme formation and associated regulatory proteins, and we also identified a novel role of the PBAC1 proteasome assembly chaperone in seed coat development.

Full Text

This preprint is available for download as a PDF.

Table

Due to technical limitations, table 1 is only available as a download in the Supplemental Files section.

Figures

Figure 1

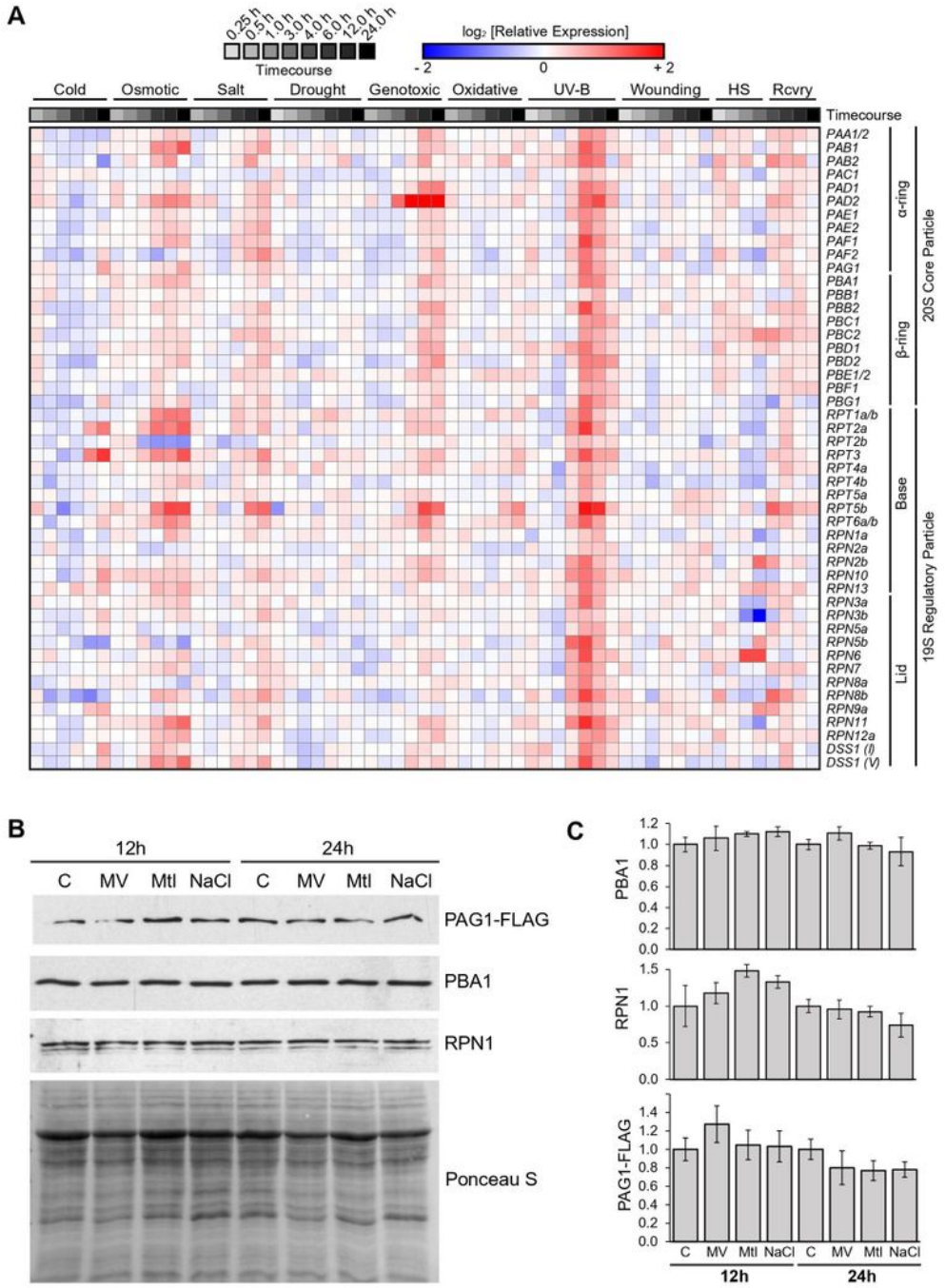

Figure 1

Effect of abiotic stresses on expression and steady-state level of proteasome subunits. (A) Microarray data of Arabidopsis seedlings exposed to cold (4oC), osmotic (300 mM mannitol), salt (150 mM NaCl), drought (air stream), genotoxic (1.5 µg/ml bleomycin), oxidative (10 µM methyl viologen), UV-B, wounding, and heat shock (38oC) stresses from Kilian et al. (2007) were obtained via the BAR Expression Browser (http://bar.utoronto.ca/) and organized into a heat map using Morpheus (broadinstitute.org).

Heat map displays log2-transformed expression-fold changes with min/max cut-off values of -2/+2. Note that for heat stress, the 4.0- to 24.0-hour time points represent variable 25oC recovery times (Rcvry) following an initial 3.0-hour heat shock (HS) at 38oC. (B) Eight-day-old PAG1-FLAG seedlings were exposed 10 μM methyl viologen (MV), 300 mM mannitol (Mtl), and 150 mM NaCl for 12 and 24 hours. Anti-FLAG, anti-PBA1, and anti-RPN1 immunoblots of PAG1-FLAG total lysates were resolved on 12% SDS-PAGE, highlighting representative subunits of the CP α-ring, β-ring, and RP lid, respectively. Loading was normalized based on fresh weight and a Ponceau S stain is included as a loading control. It should be noted that the overall protein profiles as revealed by Ponceau S staining in B for either 12- or 24-hour treatments are comparable suggesting viable seedlings. Three biological replicates were performed, and quantification of protein levels is shown in (C).

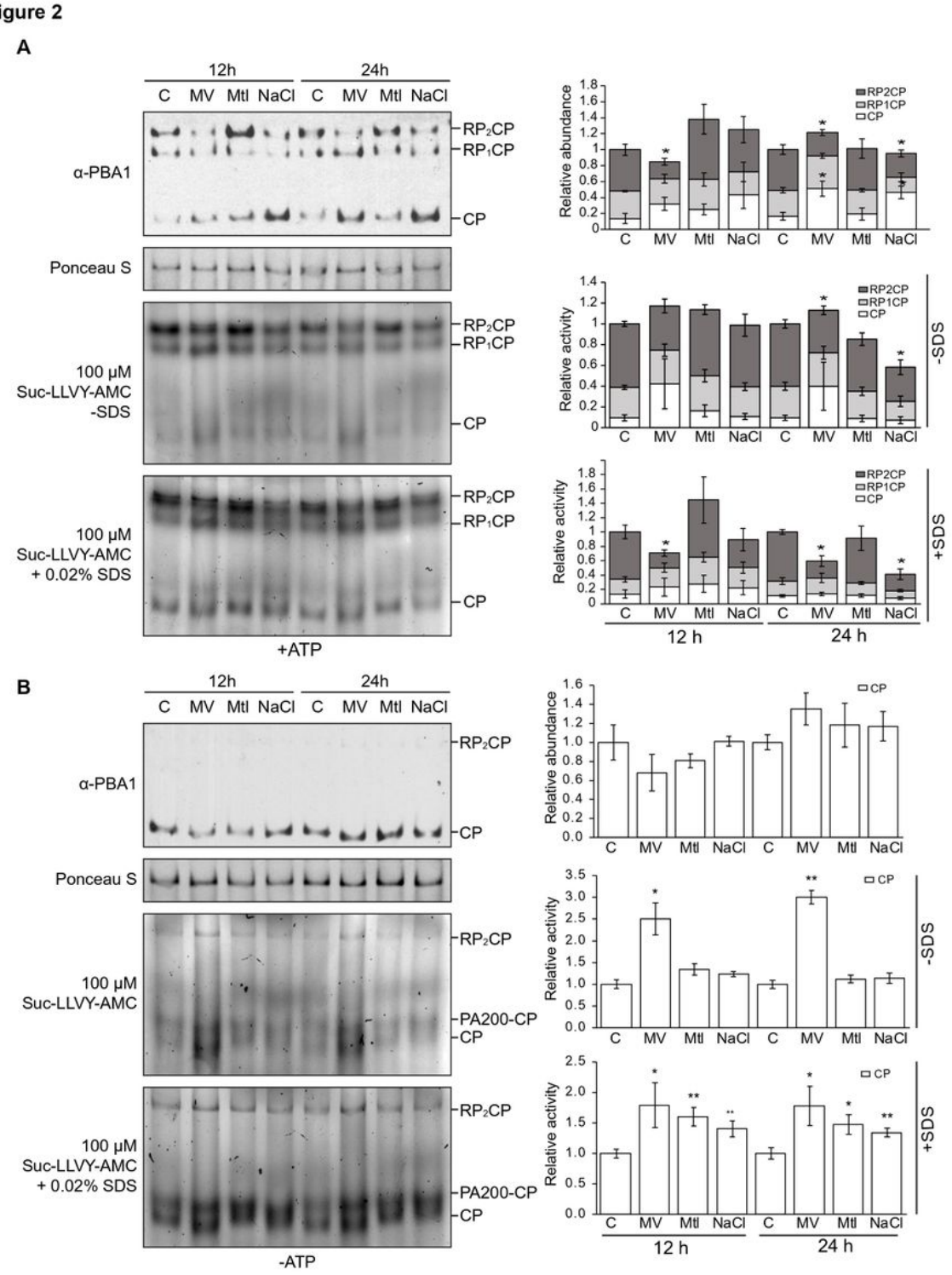

Figure 2

Oxidative and salt stresses change the stoichiometry of proteasome complexes and alter activities of CP. (A, B) Anti-PBA1 immunoblot and Suc-LLVY-AMC (100 μM) stain of total lysates resolved on 4% Native-PAGE showing abundance and peptidase activity of the proteasome particles, respectively. PAG1-FLAG seedlings were stress-treated for 12 and 24 hours before lysis in extraction buffers with (A) and without (B) 20 mM ATP. Loading was normalized based on fresh weight and a Ponceau S stain is included as a

loading control. 0.02% SDS was used to artificially activate the free 20S CP. Three biological replicates were conducted, and one is shown. Bar graphs show digital quantifications of band intensities from immunoblots or activity gels. Data is expressed relative to the control for each time point, which is arbitrarily assigned a total signal value of 1.0. For Native-PAGE run with exogenous ATP, quantifications of RP2CP, RP1CP, and free CP are expressed as a fraction of total sample signal within stacked bars. All bar charts display the means of three biological replicates ± SEM. Significant differences in RP2CP, RP1CP or free CP signal between control and stress conditions were determined by independent Student's t-tests (* = $p < 0.05$, ** = $p < 0.01$). It should be noted that in B only trace R1CP and R2CP signals were shown in this representative Western blotting image and this particularly exposure was chosen to best maintain the free CP signals in linear range.

Figure 3

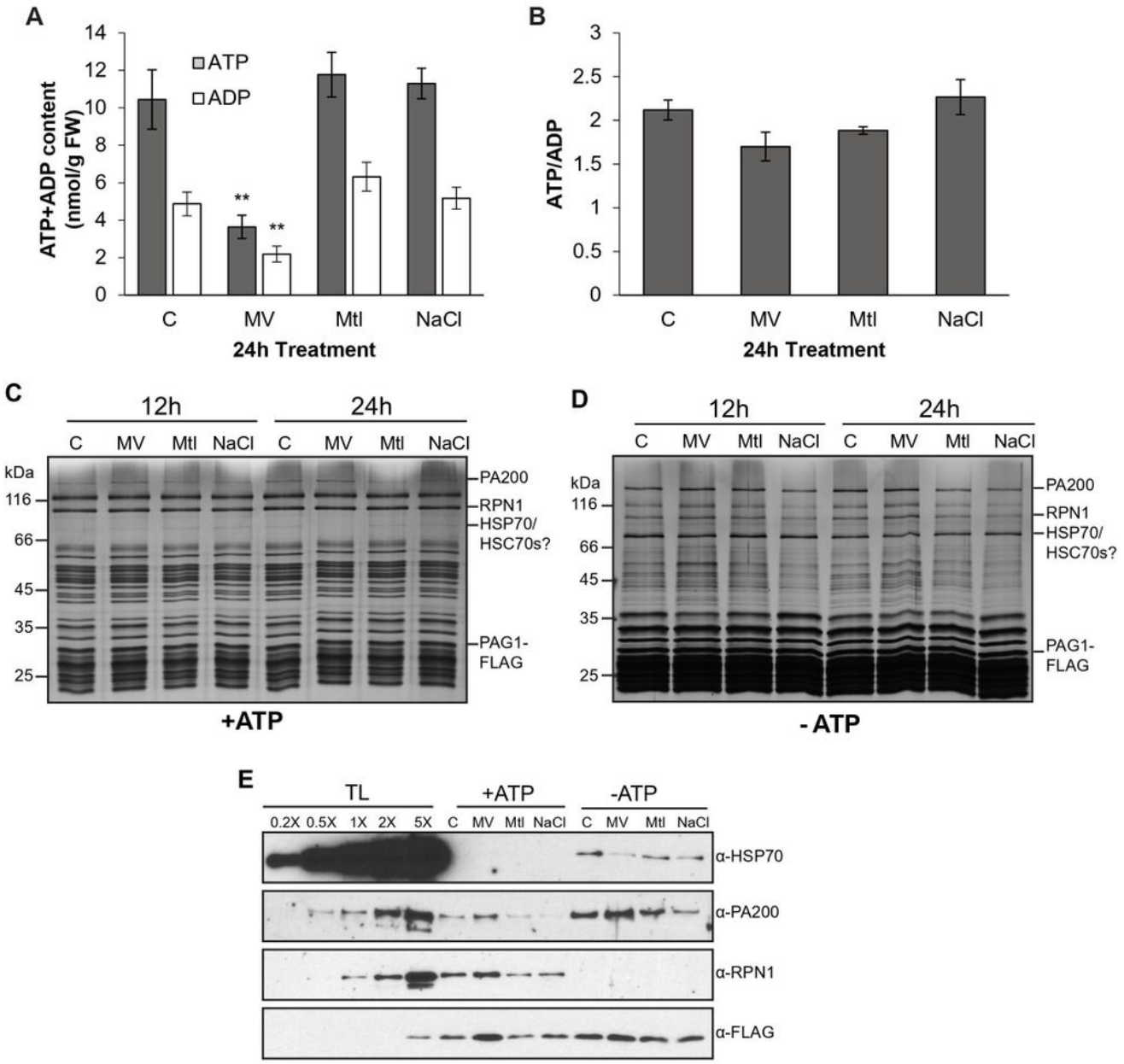

Figure 3

Cellular ATP contents and extrinsic proteasome-associated proteins are affected by oxidative and salt stresses. (A, B) Cellular levels of ATP, ADP (A) and ATP/ADP ratio (B) of PAG1-FLAG seedlings stress-treated for 24 hours. Data are displayed as means ± SEM of six biological repeats. Significant differences between control and stress conditions were determined by independent Student's t-tests (*=p <0.05, ** = p < 0.01). (C, D) Co-immunoprecipitation (Co-IP) of PAG1-FLAG-tagged proteasomes from 12- and 24-hour

stress-treated seedlings via M2 anti-FLAG antibody resin. Cell lysis and co-IP were performed in the presence (C) and absence (D) of 20 mM ATP. Eluates are visualized on a silver-stained 12% SDS-PAGE gel. (E) Immunoblotting analysis with anti-HSP70, anti-FLAG, anti-RPN1, and anti-PA200 antibodies performed on Co-IP eluates from the 12-hour time point shown in (C, D). For the immunoblots, Co-IP eluates were loaded alongside increasing concentrations of total lysate (TL) obtained from the 12-hour control (C) sample (+ATP).

Figure 4.

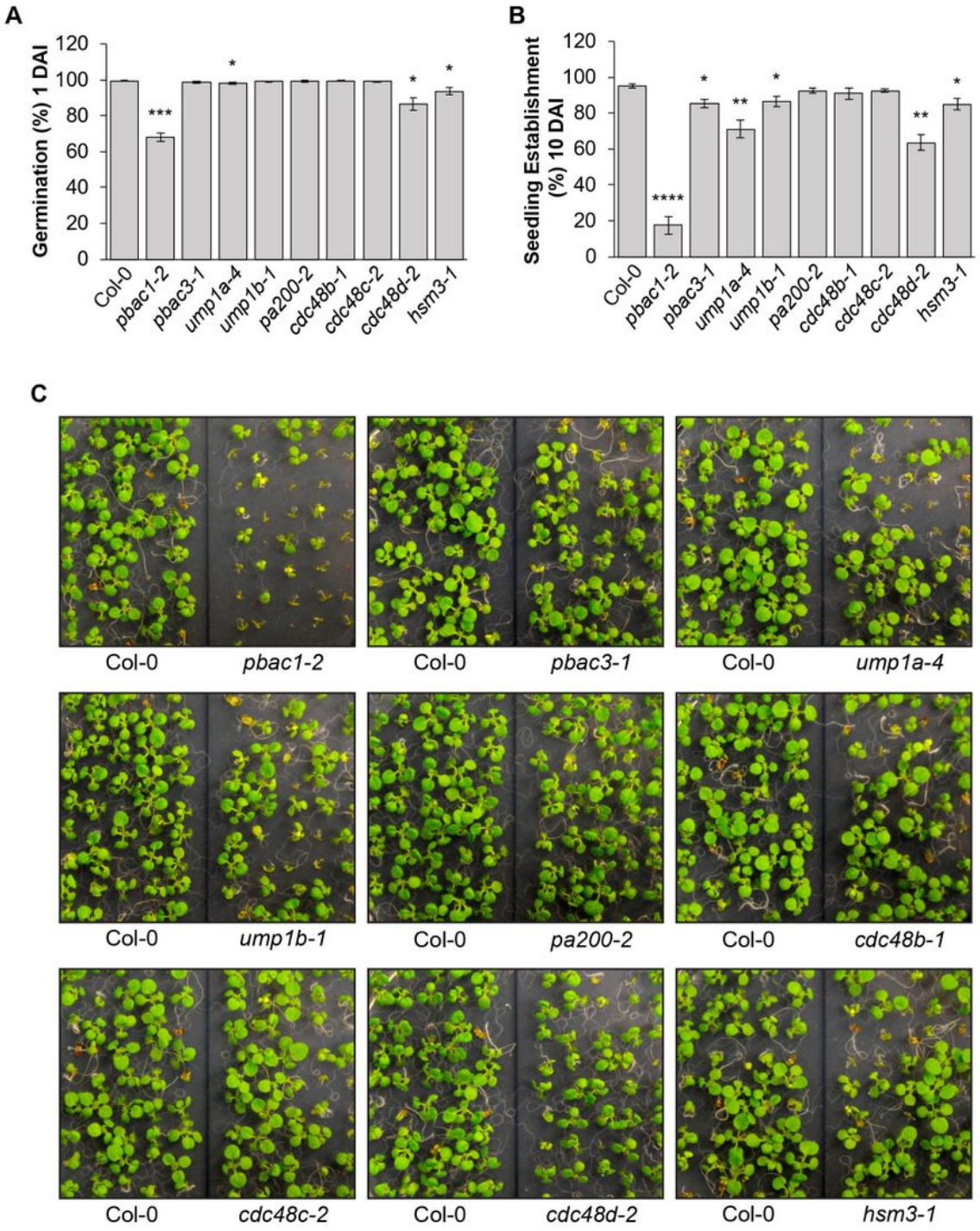

Figure 4

T-DNA insertion mutants in proteasome-associated proteins (PAPs) display arrested or delayed seedling growth. (A, B) Seed germination (radicle protrusion) and seedling establishment (seedlings that showed at least four true leaves) rates were quantified at 1 and 10 days after imbibition (DAI), respectively. Bar charts express the mean ± SEM of five biological repeats (n = 124 seedlings). Independent Student's t-tests were used to assess statistical significance of differences between each mutant and Col-0 (* =p<0.05, ** = p<0.01, **** = p<0.001). (C) Images of Col-0 and homozygous pbac1-2, pbac3-1, ump1a-4, ump1b-1, pa200-2, cdc48b-1, cdc48c-2, cdc48d-2, and hsm3-1 mutants grown on half-strength MS media for 10 DAI.

Figure 5.

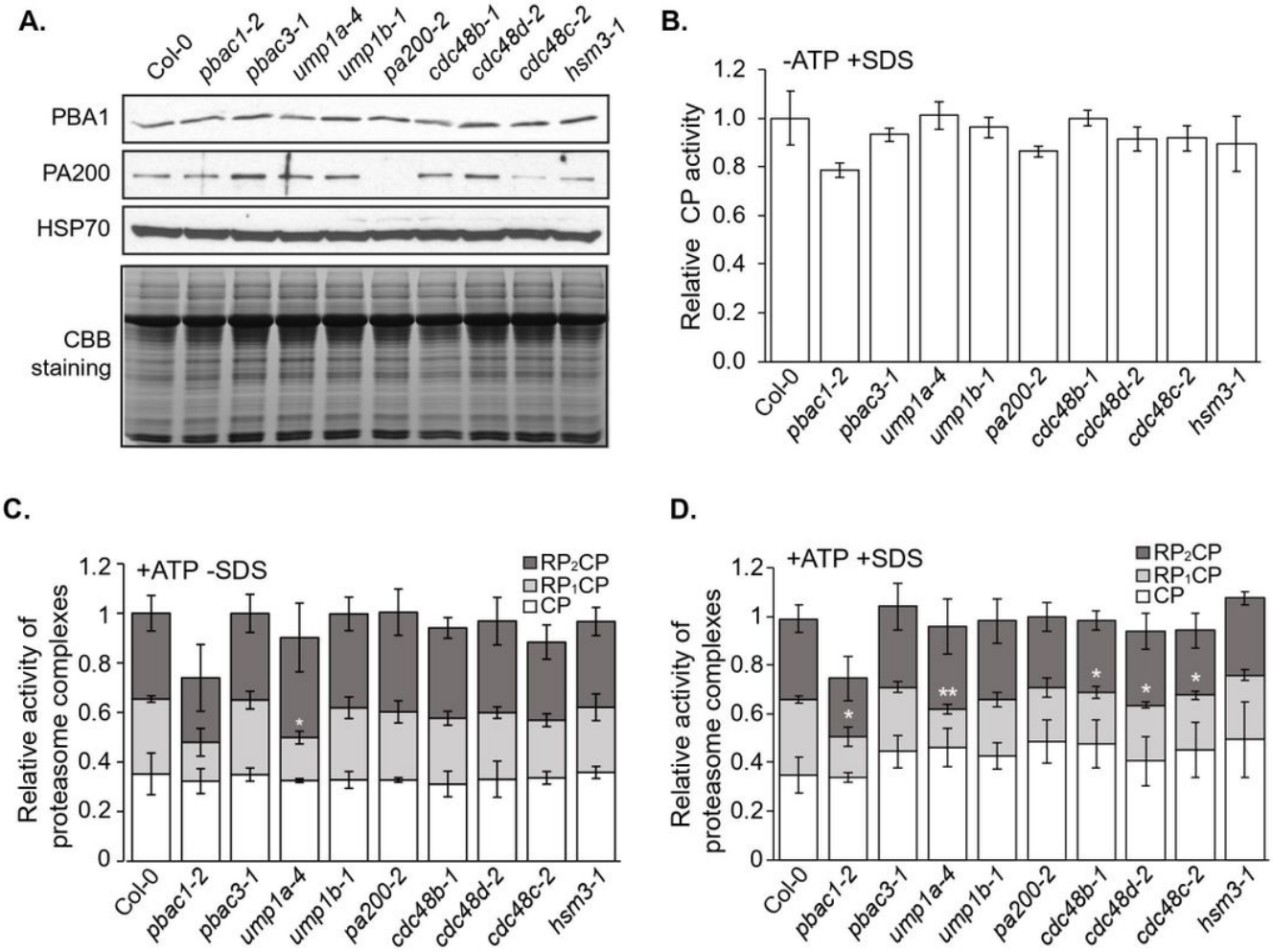

Figure 5

Decreased activity of the RP1CP species in proteasome-associated protein (PAP) mutants. pbac1-2, pbac3-1, ump1a-4, ump1b-1, pa200-2, cdc48b-1, cdc48c-2, cdc48d-2, and hsm3-1 mutants were grown for 10 days on half-strength MS media as shown in Fig. 4C. (A) Anti-PBA1, anti-PA200, and anti-HSP70

immunoblots of PAP mutant lysates resolved on 12% SDS-PAGE. (B) Quantitative analysis of Suc-LLVY-AMC (100 μM) stain signals of total lysates prepared and resolved on 4% Native-PAGE without any exogenous ATP. (C, D) Quantitative analysis of Suc-LLVY-AMC (100 μM) stain signals of total lysates prepared with 20 mM ATP and resolved on 4% Native-PAGE with 1 mM ATP. The native gels were stained and quantitated without (C) or with (D) incubation of 0.02% SDS to artificially activate the 20S CP. All mutant signals are expressed relative to that of Col-0, which is arbitrarily assigned a total signal value of 1.0. For gels run with exogenous ATP, quantifications of RP2CP, RP1CP, and free CP are expressed as a fraction of total sample signal within stacked bars. All bar charts display the means of three biological replicates ± SEM. Significant differences in RP2CP, RP1CP or free CP signal between each mutant and Col-0 were determined by independent Student's t-tests (* = $p < 0.05$, ** = $p < 0.01$).

Figure 6.

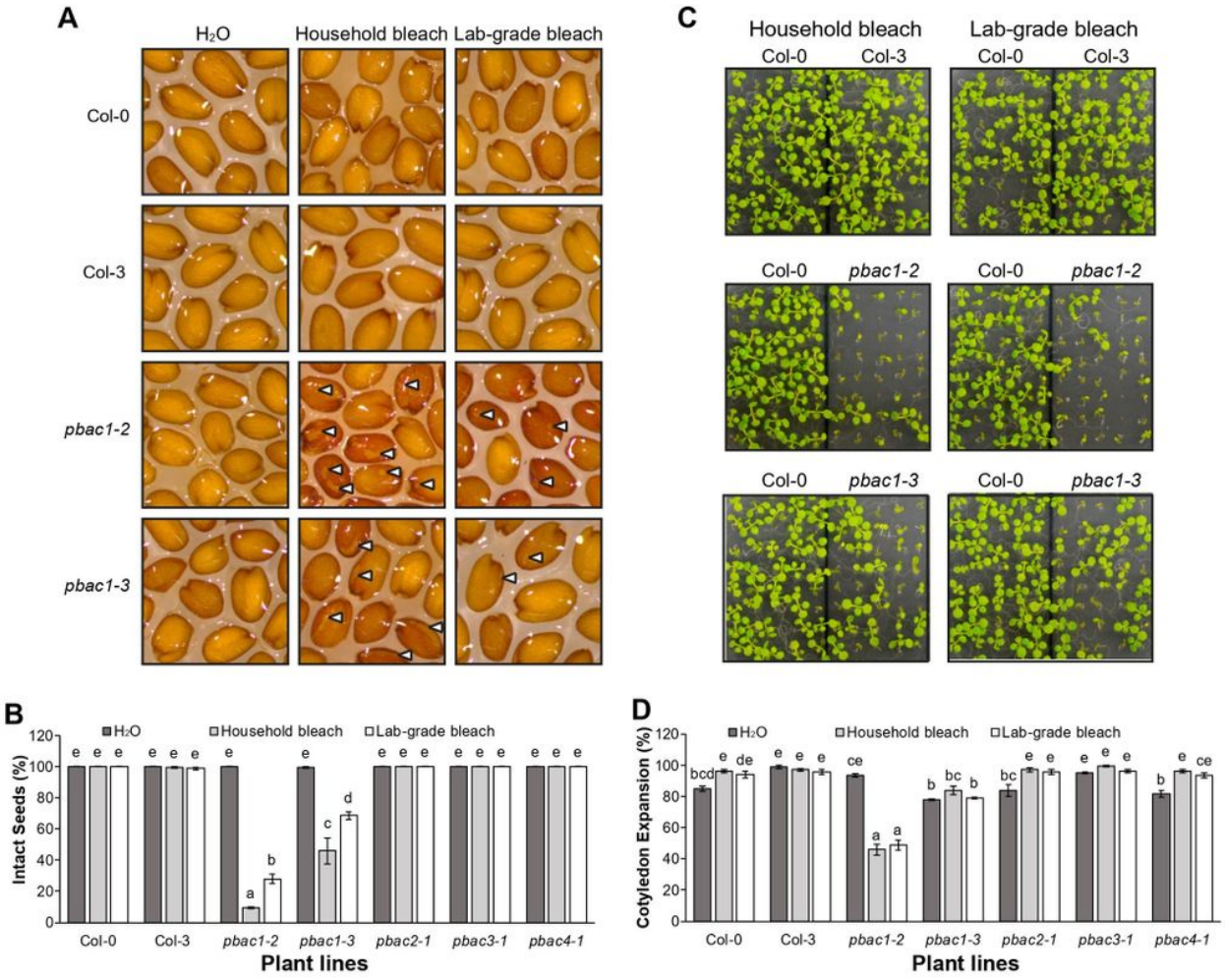

Figure 6

Darkening and tearing of pbac1 seed coat following sterilization with bleach. Dry seeds were either imbibed in H2O (non-sterile), household bleach (LAVO-12; 2.58% NaOCl), or laboratory-grade bleach (BioShop; 2.58% NaOCl). (A) Enlarged images of Col-0, Col-3, pbac1-2 and pbac1-3 seeds following treatment. Holes in the seed coat are indicated by white arrowheads. (B) Proportion of treated seeds without visible holes, namely intact seeds (C) Images of Col-0, Col-3, pbac1-2, and pbac1-3 seeds that had been treated with household or lab-grade bleach and then grown on half-strength MS media for 10 DAI. Note that non-sterile seeds could not be grown to this stage due to contamination. (D) Proportion of treated seedlings with expanded cotyledons at 3 DAI. Bar charts display the means of three biological repeats (n = 50 seeds and n = 56 seedlings, respectively) ± SEM. Means that do not share a common letter differ significantly ($p < 0.05$) as analyzed by two-way ANOVA and Tukey's HSD test. Note that pbac1-2 and pbac1-3 mutations are in the Col-3 ecotype. The remainder of the mutants are in the Col-0 ecotype.

Figure 7

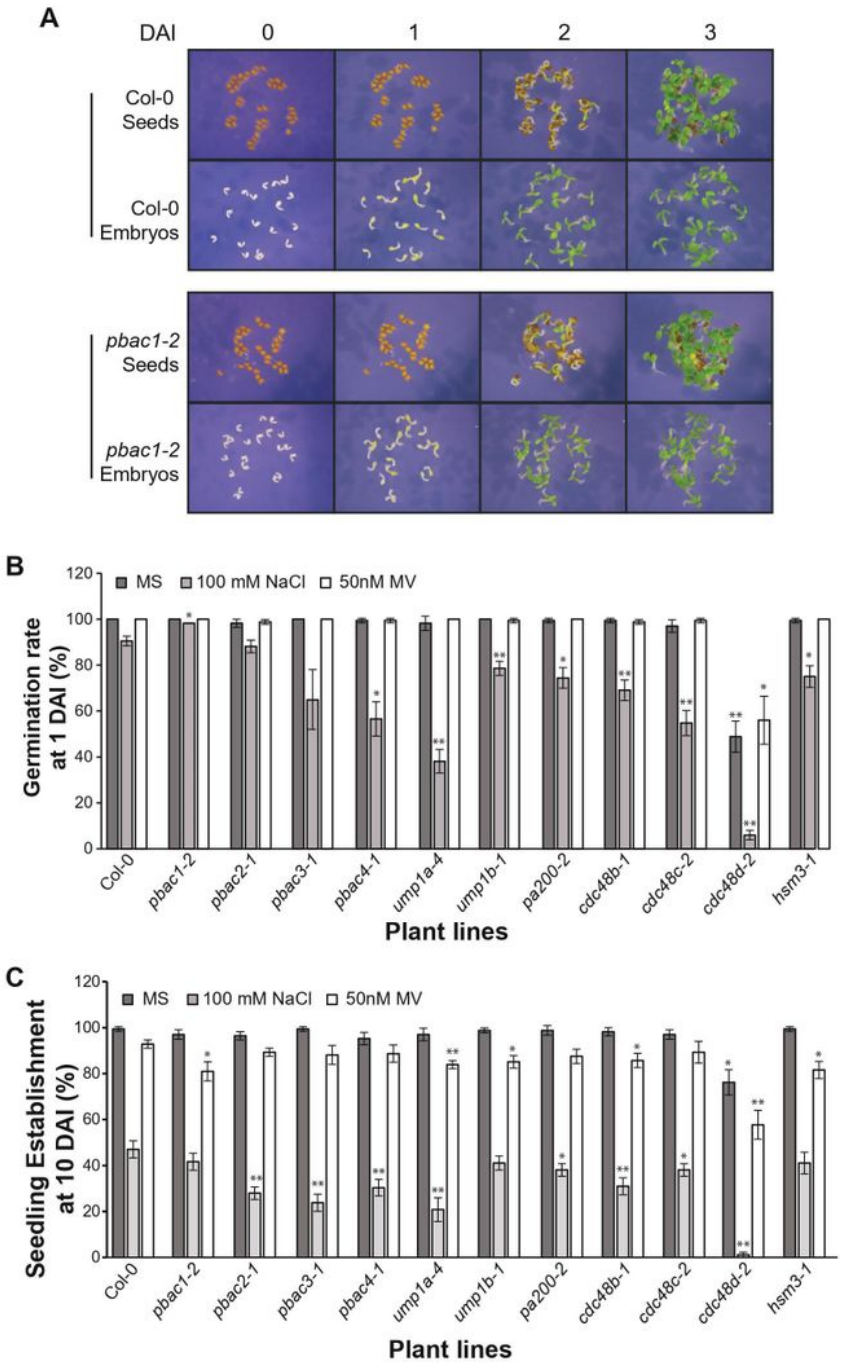

Figure 7

Germination and seedling development of PAP mutants under salinity and oxidative stresses without bleach sterilization. (A) Images of non-sterile whole seeds or dissected embryos from Col-0 and pbac1-2 lines sown on half-strength MS media from 0-3 DAI. (B, C) Germination rate at 1 DAI (B) and seedling establishment at 10 DAI (C) of wild type (Col-0) and PAP mutant seeds on half-strength MS media (MS), 100 mM NaCl or 50 µM MV. Bar charts display the means of three biological repeats (n = 56 seeds and n

= 56 seedlings, respectively) ± SD. Student's t-test with two-tailed distribution and two-sample unequal variance was performed for each mutant line and the Col-0 was used as reference. *= $p<0.05$ and **= $p<0.01$, respectively.

Figure 8

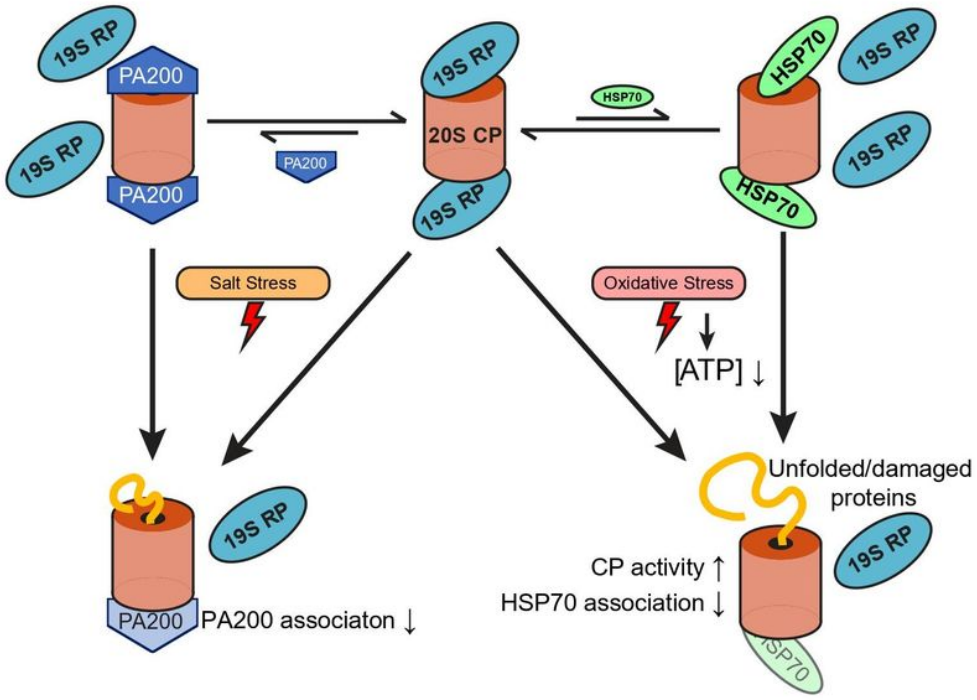

Figure 8

Model of proteasome dynamics under oxidative and salt stresses. Cellular 26S proteasome is dynamically assembled and disassembled from 19S RP and 20S CP, and associates with chaperones such as HSP70, as well as alternate caps, including PA200. Oxidative and salt stresses both diminish the association between the 19S RP and the 20S CP, and oxidative stress may trigger 26S proteasome dissociation indirectly through a reduction in cellular ATP content. Activity of the dissociated or free 20S proteasome is increased under oxidative stress, possibly due to its greater propensity for the open state or higher affinity to oxidized and misfolded proteins. While the 20S proteasome also exhibits reduced association with HSP70s under oxidative stress, salt stress causes decreased interaction with proteasome associated proteins, such as PA200. Note that the proteasome particles and associated proteins are not drawn in scale.

Supplementary Files

This is a list of supplementary files associated with this preprint. Click to download.

- Originalfulllengthblots.pdf
- FigureS1S8.pdf
- TableS1Arabidopsislinesusedinthisstudy.xlsx
- TableS2Primersusedinthisstudy.xlsx
- TableS3RawMSdataforallidentifiedproteins.xlsx
- TableS4MassSpecTablesNormalizedTotalSpectraforPAPs.xlsx
- Table1Summaryof26Sproteasome.pdf